Power Engineering and Engineering Thermophysics
https://www.acadlore.com/journals/PEET

Magnetic Field Impacts on Nanofluid Flow Towards a Stretching Sheet Embedded in a Porous Medium with Considerations of Variable Viscosity and Convective Boundary Conditions

Murali Gundagani[1*], Venkata Narendra Babu N[2]

[1] Department of Mathematics, Sreenidhi University, 501301 Yamnampet, India
[2] Department of Mathematics, Sri Satya Sai University for Human Excellenece, 585313 Kalaburagi, India

* Correspondence: Murali Gundagani (murali.g@suh.edu.in)

Received: 08-17-2023 **Revised:** 09-15-2023 **Accepted:** 09-24-2023

Citation: M. Gundagani and V. N. Babu N, "Magnetic field impacts on nanofluid flow towards a stretching sheet embedded in a porous medium with considerations of variable viscosity and convective boundary conditions," *Power Eng. Eng. Thermophys.*, vol. 2, no. 3, pp. 162–172, 2023. https://doi.org/10.56578/peet020304.

Abstract: This investigation elucidates the intertwined effects of magnetic fields and porous media on the flow of nanofluids towards a stretching sheet, contemplating variable viscosity and convective boundary conditions. A nanofluid model, incorporating the influences of thermophoresis and Brownian motion, is adopted. Via judicious transformations, the fundamental governing coupled non-linear partial differential equations are condensed, and the consequent transformed equations are numerically resolved employing the Finite Element Method (FEM). Paramount emphasis is accorded to parameters embodying notable physical significance, inclusive of the Prandtl number (Pr), Hartmann number, Lewis number (Le), Brownian motion number (Nb), thermophoresis number (Nt), and permeability parameter. The numerical results acquired, as particular instances of the aforementioned study, are found to be congruent with previously reported findings, substantiating the accuracy and reliability of the proposed methodology. A thorough examination of the collective impact of the selected parameters on flow and heat transfer characteristics has been systematically undertaken, revealing intricate dependencies and fostering a deeper understanding of the complex phenomenon under consideration. This study, hence, paves a pathway towards bolstering the comprehension of flow mechanics in porous media under the influence of magnetic fields, contributing valuable insights to the overarching field of fluid dynamics in nano-engineering applications.

Keywords: Porous medium; Stretching sheet; Nanofluid flow; Magnetic field; Finite Element Method

1 Introduction

Rapid expansions within the realm of nanofluid fluxes literature have been observed, marking significant progress in understanding heat conduction through various mediums. Conventional fluids such as oil, water, and grease have been acknowledged as suboptimal conductors of heat, primarily due to the pivotal role thermal conductivity plays in influencing the heat transfer coefficient between the heat transfer medium and the corresponding surface. Nanofluids, comprising nanoparticles typically derived from elemental metals or their oxides, have surfaced as prominent agents in enhancing thermophysical phenomena and subsequent heat transfer performance due to their expansive surface area and inherent stability.

The paramountcy of nanoparticle characteristics – inclusive of material type, shape, and size – on the efficacy of heat transfer has been underscored, necessitating a meticulous investigation into the particulars of Brownian motion and thermophoresis, which are pivotal slip mechanics in nanofluids. Special attention has also been accorded to radiative heat transfer, executed via electromagnetic waves throughout the energy transmission process, particularly within the context of nanofluids.

The conventional narrative of radiative heat transfer, often delineated through linear models assuming a straightforward relationship between temperature differences and radiative heat flow, e.g., the Stefan-Boltzmann equation, has occasionally been supplanted by non-linear radiative heat flow models to provide an accurate depiction of heat transfer behaviours. Notably, the incorporation of non-linear radiative heat flow compensates for the radiative attributes of the nanofluid, accounting for scattering and absorption of radiation by suspended nanoparticles. These

variables bear the potential to modulate radiative heat transfer by modifying the nanofluid's effective thermal conductivity and its absorption and emission properties.

Various approaches have been employed to describe non-linear radiative heat flow amidst the presence of a nanofluid. Substantial emphasis has been placed on nanoparticle concentration, size, and shape in radiative heat transfer calculations, facilitated by employing intricate mathematical models or numerical simulations that encapsulate the interactions between the nanoparticles and incoming radiation. The determination of the nanofluid's extinction coefficient, scattering phase function, and additional radiative properties may be achieved experimentally. Subsequent incorporation of these quantifiable traits into non-linear radiative heat transfer models augments the accuracy of projections.

Fluids, inherently capable of flowing and deforming under the application of external forces, are distinguished into various types, with non-Newtonian fluids finding myriad applications across diverse sectors such as natural products, biomedical fields, and agriculture. The burgeoning interest in non-Newtonian fluid flows, especially over the past decade, has been attributed to its extensive applicability across engineering and industrial domains.

Studies examining the impact of convective boundary condition on nanofluid flow past a stretching sheet have been presented by Makinde and Aziz [1], while effects of partial slip on stagnation point over a nanofluid towards a stretching surface were explored by Nadeem et al. [2]. Research conducted by Ibanez [3], investigated the magnetohydrodynamic flow past a porous channel considering entropy generation and convective boundary conditions. RamReddy et al. [4] analysed mixed convective flow of nanofluid in the presence of a convective boundary condition.

Further studies encompassing considerations for magnetic field and convective boundary condition in 3D flow in the presence of a couple stress nanofluid past a non-linearly stretching surface were discussed by Hayat et al. [5]. Thermal radiative flow of magneto water-based nanofluid past a nonlinearly stretching surface was studied by Mahanthesh et al. [6], while Aziz [7] focused on stagnation point over a hyperbolic tangent nanofluid flow with convective conditions. Subsequent studies by Ishak [8] and López et al. [9] explored similarity solutions over a flat plate and analytical solutions for heat transfer flow past a permeable surface with a convective boundary condition, respectively. Buongiorno [10] emphasized the entropy generation analysis of MHD nanofluid flow in a porous vertical microchannel.

Concurrent research avenues explored by the studies [11–23] delved into heat and mass transfer effects, providing substantial insight into the nature of the work reported. Additionally, the studies [24–30], which explored finite element solutions for heat and mass transfer problems and analysed various effects, have been instrumental in shaping understanding and analytical methodologies within the domain.

This corpus of existing research serves as a catalyst, steering the primary focus of the present article towards an exhaustive exploration of the amalgamated impact of magnetic field and porous medium on non-Newtonian nanofluid flow over a nonlinear stretching surface, concomitant with variable viscosity and convective boundary conditions. Brownian motion and thermophoresis effects have been scrutinized, with the non-linear system comprehensively computed through the FEM. Comprehensive analyses, elucidating fluid velocity, temperature, and nanoparticle concentration profiles for various governing parameters, have been graphically delineated.

2 Mathematical Formulation

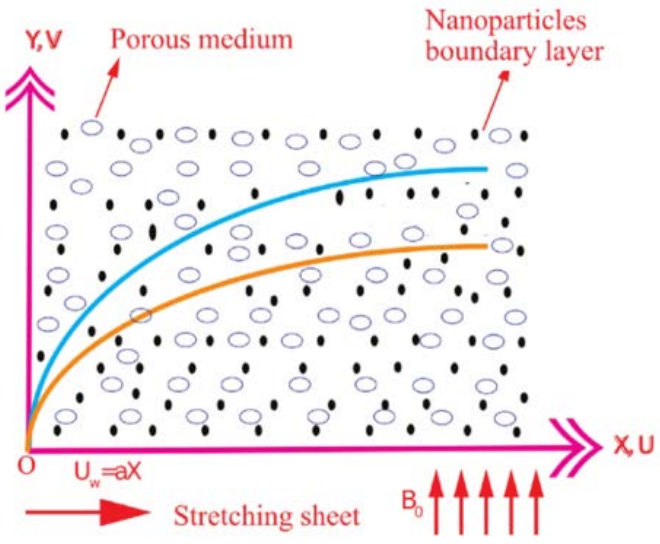

Figure 1. Geometry of the problem

A two-dimensional, steady, viscous, incompressible, electrically conducting, and laminar nanofluid flow past a stretching surface, accompanied by variable viscosity and a convective boundary condition, is considered in the present examination. The geometrical framework pertinent to this research is elucidated in Figure 1.

In the adaptation of the model proffered by Buongiorno [10], the subsequent governing equations are formulated:

Continuity Equation:

$$\left(\frac{\partial u}{\partial x}\right)+\left(\frac{\partial v}{\partial y}\right)=0 \tag{1}$$

Momentum Equation:

$$u\left(\frac{\partial u}{\partial x}\right)+v\left(\frac{\partial u}{\partial y}\right)=-\frac{1}{\rho_f}\left(\frac{\partial p}{\partial x}\right)+v\left(\frac{\partial^2 u}{\partial x^2}+\frac{\partial^2 u}{\partial y^2}\right)-\left(\frac{\mu}{k^*}\right)u-\left(\frac{\sigma B_o^2}{\rho_f}\right)u \tag{2}$$

$$u\left(\frac{\partial v}{\partial x}\right)+v\left(\frac{\partial v}{\partial y}\right)=-\frac{1}{\rho_f}\left(\frac{\partial p}{\partial y}\right)+v\left(\frac{\partial^2 v}{\partial x^2}+\frac{\partial^2 v}{\partial y^2}\right) \tag{3}$$

Equation of Thermal Energy:

$$\begin{gathered}u\left(\frac{\partial T}{\partial x}\right)+v\left(\frac{\partial T}{\partial y}\right)=\alpha\left(\frac{\partial^2 T}{\partial x^2}+\frac{\partial^2 T}{\partial y^2}\right)+\\ \tau\left\{D_B\left(\left(\frac{\partial T}{\partial x}\right)\left(\frac{\partial C}{\partial x}\right)+\left(\frac{\partial T}{\partial y}\right)\left(\frac{\partial C}{\partial y}\right)\right)+\left(\frac{D_T}{T_\infty}\right)\left(\left(\frac{\partial T}{\partial x}\right)^2+\left(\frac{\partial T}{\partial y}\right)^2\right)\right\}\end{gathered} \tag{4}$$

Concentration Equation:

$$u\left(\frac{\partial C}{\partial x}\right)+v\left(\frac{\partial C}{\partial y}\right)=D_B\left(\frac{\partial^2 C}{\partial x^2}+\frac{\partial^2 C}{\partial y^2}\right)+\left(\frac{D_T}{T_\infty}\right)\left(\frac{\partial^2 T}{\partial x^2}+\frac{\partial^2 T}{\partial y^2}\right) \tag{5}$$

For the described flow, the pertinent boundary conditions are established as follows:

$$\left.\begin{gathered}u=ax, v=0, -k\left(\frac{\partial T}{\partial y}\right)=h\left(T_f-T\right), C=C_w \text{ at } y=0 \,\&\, u\to 0, T\to T_\infty, C\to C_\infty \text{ as } y\to\infty\end{gathered}\right\} \tag{6}$$

By using similarity transformations

$$\left.\begin{gathered}\eta=y\sqrt{\left(\frac{a}{v}\right)}, \psi=(\sqrt{av})xf(\eta), \theta(\eta)=\frac{T-T_\infty}{T_f-T_\infty}, \varphi(\eta)=\frac{C-C_\infty}{C_w-C_\infty}\end{gathered}\right\} \tag{7}$$

where, ψ represents the stream function, accompanied by $u=\frac{\partial\psi}{\partial y}, v=-\frac{\partial\psi}{\partial x}$, and $f'=\frac{u}{u_w}=\frac{u}{ax}$:

An order-of-magnitude analysis of the momentum equation in the direction (perpendicular to the stretching sheet), utilising conventional boundary layer approximations $u>>v\Rightarrow\frac{\partial u}{\partial y}>>\frac{\partial u}{\partial x}\cdot\frac{\partial v}{\partial x}\cdot\frac{\partial v}{\partial y}$, reveals that $\frac{\partial p}{\partial y}=0$.

Upon disregarding the pressure gradient, the governing equations and boundary conditions are reduced to the following expressions:

$$f'''+ff''-f'^2-(M+K)f'=0 \tag{8}$$

$$\theta''+\Pr f\theta'+\Pr Nb\varphi'\theta'+\Pr Nt\theta'^2=0 \tag{9}$$

$$\varphi''+\mathrm{Lef}\,\varphi'+\frac{Nt}{Nb}\theta''=0 \tag{10}$$

Consequently, the corresponding boundary conditions Eq. (6) transform as follows:

$$\left.\begin{array}{l} f(0)=0, f'(0)=1, \theta'(0)=-Bi[1-\theta(0)], \varphi(0)=1 \\ f' \to 0, \theta \to 0, \varphi \to 0 \text{ as } \eta \to \infty \end{array}\right\} \tag{11}$$

$$\left.\begin{array}{l} \mathrm{Pr}=\frac{v}{\alpha}, Le=\frac{v}{D_B}, Nb=\frac{(\rho c)_p D_B (C_w-C_\infty)}{(\rho c)_f v}, Nt=\frac{(\rho c)_p D_T (T_f-T_\infty)}{(\rho c)_f v T_\infty}, Bi=\frac{hx}{k}\sqrt{\frac{v}{a}}, \\ M=\frac{\sigma B_o^2}{a\rho}, K=\frac{ak^*}{\mu} \end{array}\right\} \tag{12}$$

$$Cf=\frac{2\tau_w}{\rho}, Nu_x=\frac{q_w x}{k\left(T_w-T_\infty\right)}, Sh_x=\frac{J_w x}{D_B\left(C_w-C_\infty\right)} \tag{13}$$

where, τ_w, q_w and J_w represent the skin-friction, heat, and mass fluxes at the surface respectively, and these quantities are defined as follows:

$$\tau_w=\mu\left(\frac{\partial u}{\partial y}\right)_{y=0}, q_w=-k\left(\frac{\partial T}{\partial y}\right)_{y=0}, J_w=-D_B\left(\frac{\partial C}{\partial y}\right)_{y=0} \tag{14}$$

Utilising Eqs. (13) and (14), the dimensionless skin-friction coefficient, alongside wall heat and mass transfer rates, are defined as follows:

$$Cf=2\,\mathrm{Re}_x^{\frac{3}{4}} f''(0), Nu_x=-\mathrm{Re}_x^{\frac{-1}{4}}\theta'(0), Sh_x=-\mathrm{Re}_x^{\frac{-1}{4}}\phi'(0) \tag{15}$$

3 Methodological Approach

Numerical modelling and simulation consistently provide a streamlined, economical, and notably efficacious pathway to procuring solutions for intricate mathematical equations. The advent of computer numerical modelling has markedly simplified problem-solving procedures. In effect, numerical models are cultivated to seamlessly coincide with the physical system, wherein the solutions can be scrutinised and validated against authentic systems. Such numerical methods pave the way for the enhancement of approaches towards the physical system and facilitate its rapid resolution. Some notable merits of the FEM technique include:

•Modelling
•Adaptability
•Accuracy
•Boundary Recognition
•Visualization

The FEM, employed in the current study, harbours potential for utilization in ensuing research due to its prodigious utility in resolving linear and nonlinear partial and ordinary differential equations across various disciplines including physics, mechanical engineering, and related domains. At the time of penning this article, it stands as one of the most adaptable numerical techniques available for conducting engineering analysis. A plethora of numerical strategies, encompassing the LU decomposition approach, the Gauss elimination method, etc., can be enlisted to decipher formulated equations.

In the FEM, the guiding principle that the problem domain may be divided into smaller, more manageable entities, referred to as "finite elements," operates as a cornerstone. These entities, possessing finite dimensions, may further be divided into smaller segments. It has been applied to elucidate a wide array of phenomena, spanning heat transmission, fluid and solid mechanics, rigid body dynamics, solid mechanics, chemical processes, electrical systems, and acoustics. A depiction of the utilization of the FEM is presented in Figure 2, serving also as an exemplar.

Equations amassed can be resolved utilizing any numerical methodology, such as the Gauss elimination method or the LU Decomposition method, among others. Each element matrix possesses an order of 8 (Square matrix). The entire flow domain is bifurcated into 1200 line elements, and post-assembly of all element equations, a matrix of order 4804 (Square matrix) is formulated. The resultant system of equations is starkly nonlinear, necessitating resolution through a robust iterative strategy. After the imposition of aforementioned boundary conditions, a system of merely 4797 equations subsists for resolution, executed via a robust Gauss elimination approach with a precision of 0.00001. Convergence criteria utilize the relative disparity between successive iterations. Once differences satisfy the stipulated precision level, convergence of the solution is assumed, and the iterative process is ceased. The Gaussian quadrature is enlisted to address integration issues. The algorithm's computer program was executed in MATLAB, installed on a PC. Additionally, shape functions for one- and two-dimensional problems may be of higher order, incorporating linear/quadratic shape functions. Nevertheless, the applicability of shape functions fluctuates from problem to problem. In the current issue, both linear and quadratic shape functions are deployed owing to their simplicity and efficacy in calculations. However, the negligible divergence in results implies that both elements furnish roughly equivalent accuracy.

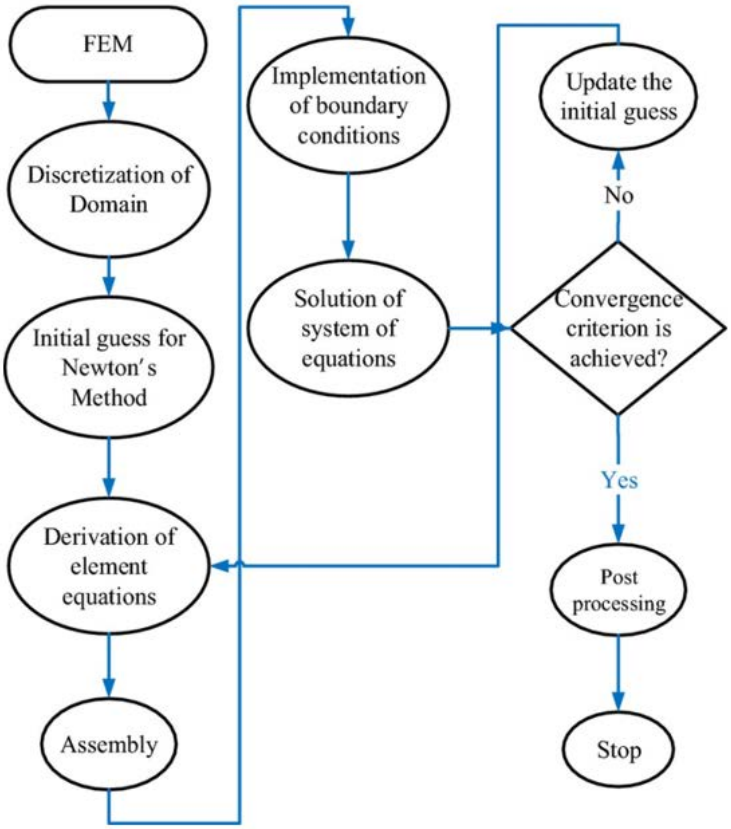

Figure 2. Illustration of the FEM via a flow chart

4 Results and Discussion

Utilising the FEM and boundary equations, the governing flow ordinary differential equations, denoted as Eqs. (8)-(10), were solved by the authors. A series of illustrative figures were developed to elucidate the impacts of various factors on equations for temperature, concentration, and dimensionless velocity, with parameter ranges predicated on aforementioned critical values. Furthermore, numerical values pertaining to skin-friction, rate of heat, and mass transfer coefficients (Nusselt and Sherwood numbers) were delineated in tabular forms for variant physical parameters.

In Figure 3, a discernible decrement in the velocity profile is observed with augmenting Hartmann numbers. Enhanced velocity profiles, attributed to diminished friction force, are indicated by Figure 4 upon increasing the permeability value (K) of the porous medium. Figure 5 illustrates an elevation in the temperature profile as values of the thermophoresis parameter (Nt) increase, highlighting the pivotal role of this parameter in scrutinizing temperature profiles across various nanofluid flow dilemmas. An appreciable escalation in the temperature profile and the accompanying boundary layer thickness with increasing Brownian motion parameter (Nb) values is demonstrated in Figure 6.

A conspicuous decline in temperature distribution with an enhanced Prandtl number (Pr) is observed in Figure 7, while Figure 8 notes an elevation in temperature profiles throughout the fluid regime as the Biot number (Bi) increases. Figure 9 illustrates a substantial reduction in nanoparticle concentration dispersion as the Lewis number (Le) increases, with the Brownian diffusion coefficient identified as a crucial determinant of Le. The graph of nanoparticle volume fraction $\phi(\eta)$ vs η in Figure 10 and Figure 11 delineate the growth of the graph and the boundary layer thickness for the nanoparticle volume fraction and fluctuations in the Brownian motion parameter (Nb), respectively.

In the context of skin-friction, mass transfer, and heat transfer coefficients:

Increasing values of the magnetic parameter (M), Lewis number (Le), and Prandtl number were observed to diminish the skin-friction coefficient, while opposite effects were noted with elevated values of the porous medium parameter (K), thermophoresis parameter (Nt), Brownian motion parameter (Nb), and Biot number (Bi). An increment in Nusselt number with increasing Thermophoresis parameter (Nt), Brownian motion parameter (Nb), and Biot number (Bi), and a decrement with escalating Prandtl number (Pr) are documented. Furthermore, the Sherwood number is identified as an increasing function of Thermophoresis parameter (Nt) and Brownian motion parameter (Nb), yet a decreasing function of Lewis number (Le).

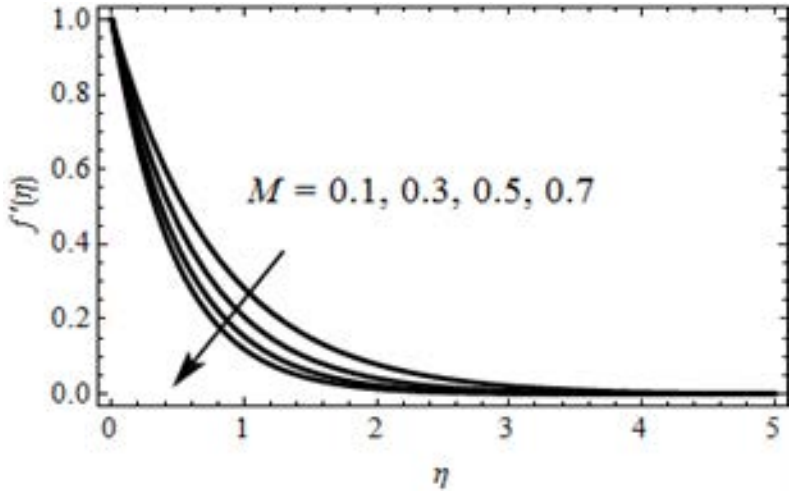

Figure 3. Influence of magnetic parameter M on velocity profiles

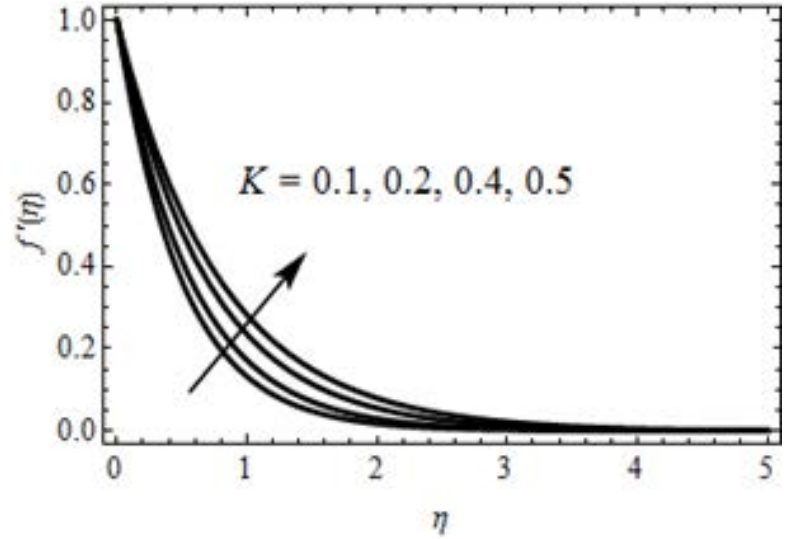

Figure 4. Permeability value K impact on velocity profiles

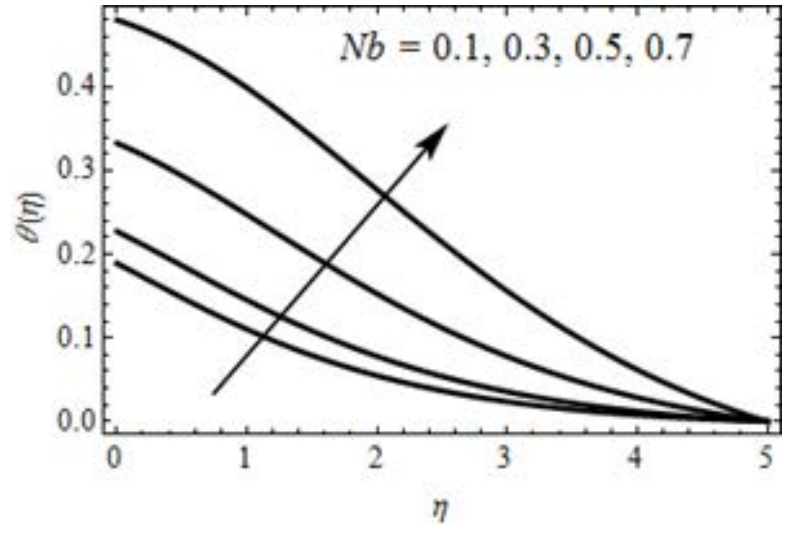

Figure 5. Brownian motion parameter Nb impact on temperature profiles

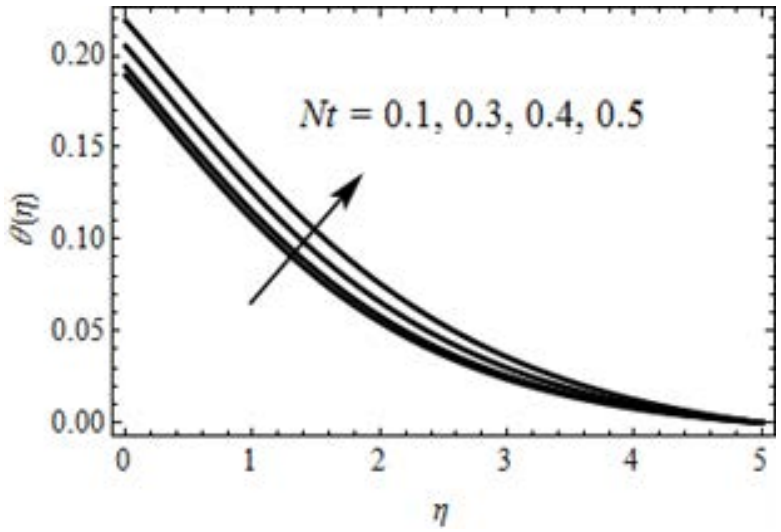

Figure 6. Thermophoresis parameter Nt influence on temperature profiles

Table 1. Comparative analysis of Nusselt number outcomes: Present study vs. studies M = K = Nb = Nt = 0 and Bi = 1000

Pr	**Present Results**	**Khan and Pop** [11]	**Wang** [12]	**Gorla and Sidawi** [13]
0.07	0.06643821578	0.0663	0.0656	0.0656
0.20	0.16852206244	0.1691	0.1691	0.1691
0.70	0.44562215487	0.4539	0.5349	0.4539
2.00	0.90123326594	0.9114	0.9114	0.9114
7.00	1.88520014562	1.8954	1.8905	1.8954
20.0	3.34203362159	3.3539	3.3539	3.3539

Table 2. Comparative analysis of Nusselt number outcomes across different values: Present study vs. studies Le = Pr = 20 and study $Bi \to \infty$

Nb	***Nt***	**Present Results**	**Khan and Pop** [11]
0.1	0.1	0.94221005487	0.9524
0.2	0.1	0.50555218845	0.5056
0.3	0.1	0.24663998744	0.2522
0.1	0.2	0.68200154489	0.6932
0.1	0.3	0.51302263408	0.5201

Table 3. Comparative analysis of Sherwood number results: Present study vs. studies Le = Pr = 20 and study $Bi \to \infty$

Nb	***Nt***	**Present Results**	**Khan and Pop** [11]
0.1	0.1	2.12882154789	2.1294
0.2	0.1	2.37620154625	2.3819
0.3	0.1	2.41002154872	2.4100
0.1	0.2	2.26920154862	2.2740
0.1	0.3	2.52031457867	2.5286

Table 1 presents a comparison of current Nusselt number results with those of Khan and Pop [11], Wang [12], and Gorla and Sidawi [13] for different values of Pr when $M = K = Nb = Nt = 0$ and Bi = 1000. Further discussions regarding the comparison of Nusselt and Sherwood number results with Khan and Pop [11] for varying values of Nb and Nt when Le = Pr=20 and $Bi \to \infty$ are unidentified, are illustrated in Table 2 and Table 3. From the aforementioned tables, it is inferred that not only are the present results in excellent alignment with existing studies but they also substantiate the efficacy of the implemented methodology.

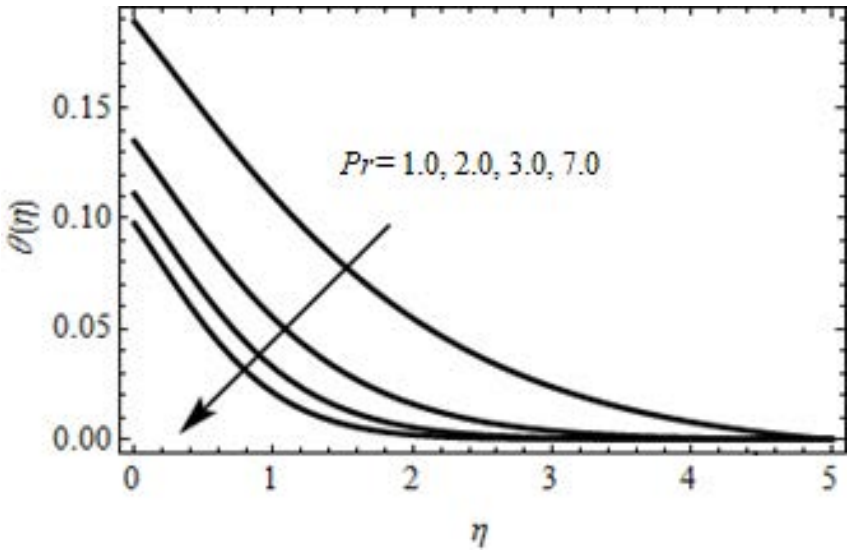

Figure 7. Impact of Prandtl number Pr on temperature profiles

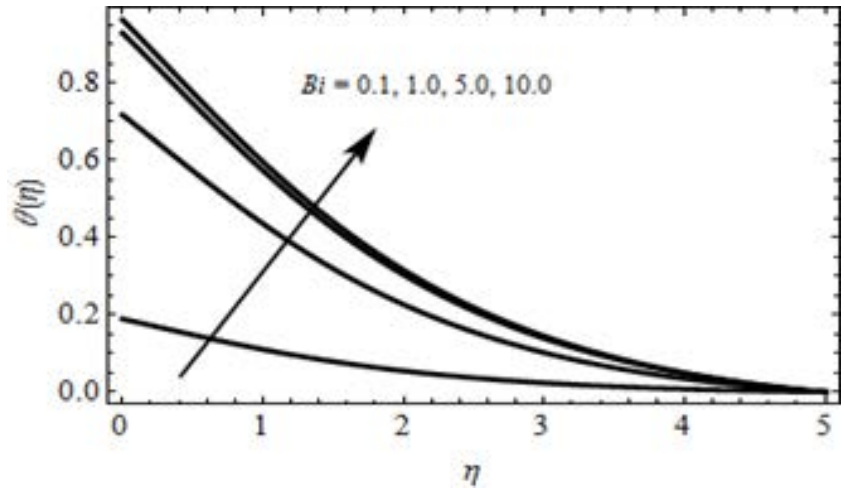

Figure 8. Temperature profiles affected by varying Biot number Bi

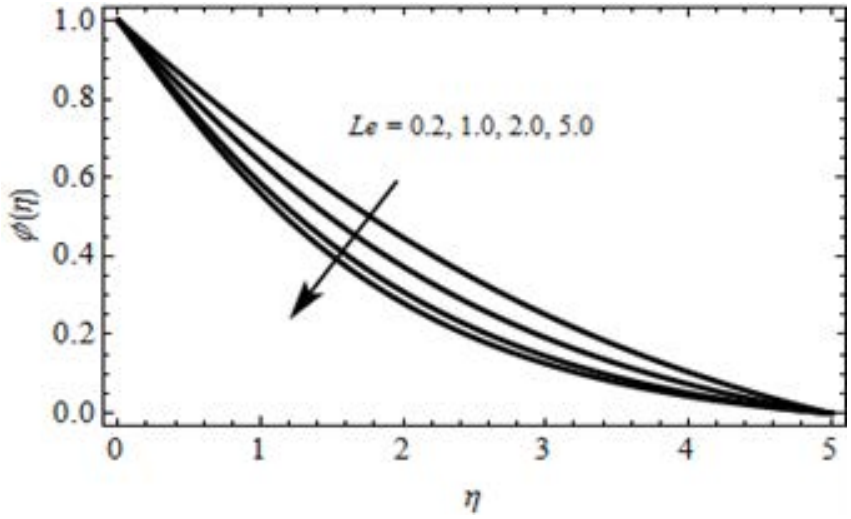

Figure 9. Influence of Lewis number $Leon$ nanoparticle concentration dispersion profiles

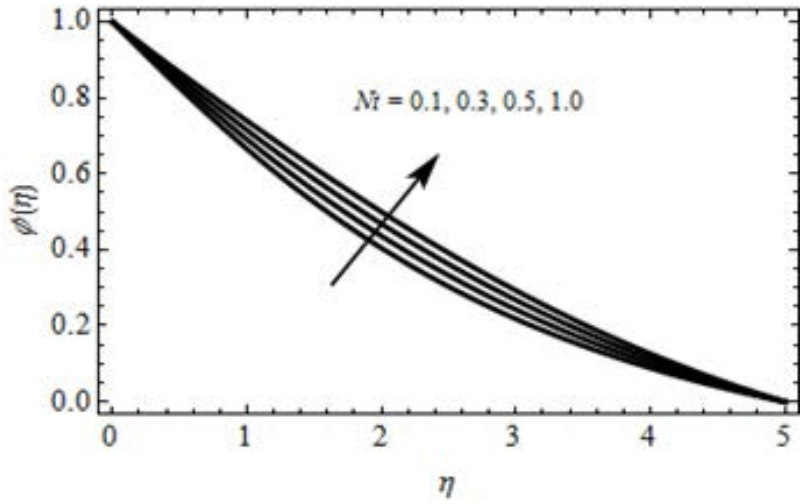

Figure 10. Thermophoresis parameter Nt and its impact on nanoparticle volume fraction $\phi(\eta)$ profiles

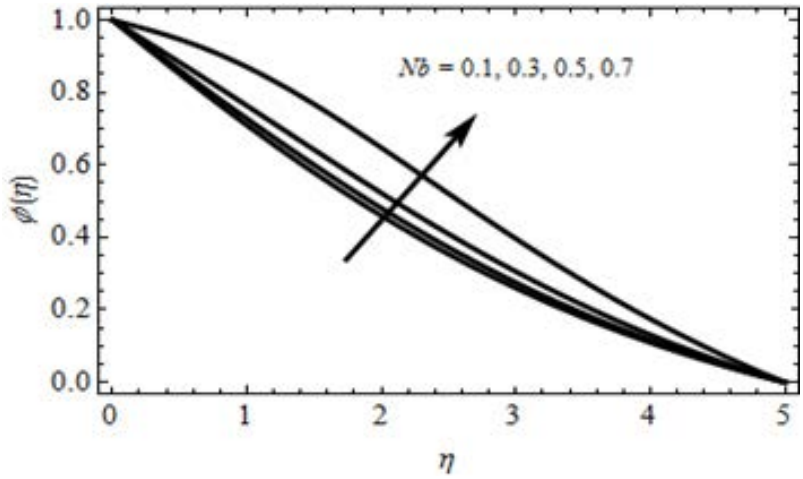

Figure 11. Impact of Brownian motion parameter Nb on concentration profiles and boundary layer thickness

5 Conclusions

An exhaustive numerical parametric investigation was conducted to elucidate the numerical interpretations of a category of nonlinear equations, aiming to delineate the solution details and to offer an in-depth analysis concerning the influence of various factors, notably the nanofluid properties and other relevant parameters, upon flow variables. The insights derived from these findings have been cogently visualised through graphical representations, facilitating a lucid and insightful comprehension of the elements involved in this study. The numerical examination of the boundary layer viscous flow and heat transfer of a non-Newtonian nanofluid over a non-linearly stretching sheet, in the presence of variable viscosity and convective boundary condition effects, was performed, revealing the following results:

•An augmentation in the magnetic parameter (M) was associated with a reduction in the velocity profile, attributable to the Lorentz force.

•Elevations in the Brownian motion parameter (Nb) and the thermophoresis parameter (Nt) were corresponded with increases in both temperature and concentration profiles.

•An increment in the Lewis number (Le) was linked with a decrease in concentration.

It was discerned that the outcomes derived from the current investigation were in congruence with previous works executed by Khan and Pop [11], Wang [12], and Gorla and Sidawi [13].

Future Research Directions:

The FEM, utilised in this investigation, is earmarked for prospective use in forthcoming research, attributed to its pronounced efficacy in solving both linear and nonlinear partial, as well as ordinary differential equations in various domains including physics and mechanical engineering. The results procured are discerned to possess a greater accuracy than those derived through alternative numerical methodologies. The FEM is presently leveraged by mechanical engineers to unravel intricate issues. Ensuing research endeavours ought to scrutinise the properties

of nanofluid flow to forge a more comprehensive understanding of transport phenomena, temperature profiles, and concentration profiles.

Data Availability

The data used to support the findings of this study are available from the corresponding author upon request.

Conflicts of Interest

The authors declare no conflict of interest.

References

[1] O. D. Makinde and A. Aziz, "Boundary layer flow of a nanofluid past a stretching sheet with a convective boundary condition," *Int. J. Therm. Sci.*, vol. 50, no. 7, pp. 1326–1332, 2011. https://doi.org/10.1016/j.ijthermalsci.2011.02.019

[2] S. Nadeem, M. Rashid, and S. A. Noreen, "Partial slip effect on non-aligned stagnation point nanofluid over a stretching convective surface," *Chin. Phys. B*, vol. 24, no. 1, 2015. https://doi.org/10.1088/1674-1056/24/1/014702

[3] G. Ibanez, "Entropy generation in MHD porous channel with hydrodynamic slip and convective boundary conditions," *Int. J. Heat Mass Transf.*, vol. 80, pp. 274–280, 2015. https://doi.org/10.1016/j.ijheatmasstransfer.2014.09.025

[4] C. RamReddy, P. V. S. N. Murthy, A. J. Chamkha, and A. M. Rashad, "Soret effect on mixed convection flow in a nanofluid under convective boundary condition," *Int. J. Heat Mass Transf.*, vol. 64, pp. 384–392, 2013. https://doi.org/10.1016/j.ijheatmasstransfer.2013.04.032

[5] T. Hayat, A. Aziz, T. Muhammad, and B. Ahmad, "Influence of magnetic field in three-dimensional flow of couple stress nanofluid over a nonlinearly stretching surface with convective condition," *PLOS ONE*, vol. 10, no. 12, p. e0145332, 2015. https://doi.org/10.1371/journal.pone.0145332

[6] B. Mahanthesha, B. J. Gireesha, and R. S. R. Gorla, "Nonlinear radiative heat transfer in MHD three-dimensional flow of water based nanofluid over a non-linearly stretching sheet with convective boundary condition," *J. Niger. Math. Soc.*, vol. 35, no. 1, pp. 178–198, 2016. https://doi.org/10.1016/j.jnnms.2016.02.003

[7] A. Aziz, "A similarity solution for laminar thermal boundary layer over a flat plate with a convective surface boundary condition," *Commun. Nonlinear Sci. Numer. Simul.*, vol. 14, no. 4, pp. 1064–1068, 2009. https://doi.org/10.1016/j.cnsns.2008.05.003

[8] A. Ishak, "Similarity solutions for flow and heat transfer over a permeable surface with convective boundary condition," *Appl. Math. Comput.*, vol. 217, no. 2, pp. 837–842, 2010. https://doi.org/10.1016/j.amc.2010.06.026

[9] A. López, G. Ibáñez, J. Pantoja, J. Moreira, and O. Lastres, "Entropy generation analysis of MHD nanofluid flow in a porous vertical microchannel with nonlinear thermal radiation, slip flow and convective-radiative boundary conditions," *Int. J. Heat Mass Transf.*, vol. 107, pp. 982–994, 2017. https://doi.org/10.1016/j.ijheatmasstransfer.2016.10.126

[10] J. Buongiorno, "Convective transport in nanofluids," *J. Heat Transf.*, vol. 128, no. 3, pp. 240–250, 2006. https://doi.org/10.1115/1.2150834

[11] W. A. Khan and I. Pop, "Boundary-layer flow of a nanofluid past a stretching sheet," *Int. J. Heat Mass Transf.*, vol. 53, no. 11-12, pp. 2477–2483, 2010. https://doi.org/10.1016/j.ijheatmasstransfer.2010.01.032

[12] C. Y. Wang, "Free convection on a vertical stretching surface," *J. Appl. Math. Mech.*, vol. 69, no. 11, pp. 418–420, 1989. https://doi.org/10.1002/zamm.19890691115

[13] R. S. R. Gorla and I. Sidawi, "Free convection on a vertical stretching surface with suction and blowing," *Appl. Sci. Res.*, vol. 52, pp. 247–257, 1994. https://doi.org/10.1007/BF00853952

[14] M. Gundagani, "Finite element solution of thermal radiation effect on unsteady MHD flow past a vertical porous plate with variable suction," *Am. Acad. Scholar. Res. J.*, vol. 4, no. 3, pp. 3–22, 2012. https://doi.org/10.9734/BJMCS/2012/1580

[15] M. C. K. Reddy, G. Murali, S. Sivaiah, and N. V. N. Babu, "Heat and mass transfer effects on unsteady MHD free convection flow past a vertical permeable moving plate with radiation," *Int. J. Appl. Math. Res.*, vol. 1, no. 2, pp. 189–205, 2012. https://doi.org/10.14419/ijamr.v1i2.502

[16] G. Murali and N. V. N. Babu, "Effect of radiation on MHD convection flow past a vertical permeable moving plate," *Int. J. Adv. Appl. Sci.*, vol. 1, no. 1, pp. 19–28, 2012.

[17] S. Sivaiah, G. Murali, M. C. K. Reddy, and R. S. Raju, "Unsteady MHD mixed convection flow past a vertical porous plate in presence of radiation," *Int. J. Basic Appl. Sci.*, vol. 1, no. 4, pp. 651–666, 2012.

[18] G. Murali, E. M. Reddy, and N. V. N. Babu, "Heat and mass transfer with free convection MHD flow past a vertical porous plate: Numerical study," *Int. J. Sci. Eng.*, vol. 8, no. 2, pp. 95–103, 2015.

[19] S. Sivaiah, G. Murali, and M. C. K. Reddy, "Finite element analysis of chemical reaction and radiation effects on isothermal vertical oscillating plate with variable mass diffusion," *ISRN Math. Phys.*, vol. 2012, p. 401515, 2012. https://doi.org/10.5402/2012/401515

[20] S. Sheri, M. Gundagani, and M. P. Karanamu, "Analysis of heat and mass transfer effects on an isothermal vertical oscillating plate," *Walailak J. Sci. Technol.*, vol. 9, no. 4, pp. 407–415, 2012.

[21] M. Gundagani, S. Sheri, A. Paul, and M. C. K. Reddy, "Radiation effects on an unsteady MHD convective flow past a semi-infinite vertical permeable moving plate embedded in a porous medium with viscous dissipation," *Walailak J. Sci. Technol.*, vol. 10, no. 5, pp. 499–515, 2013.

[22] D. Gadipally and M. Gundagani, "Analysis of Soret and Dufour effects on unsteady MHD flow past a semi infinite vertical porous plate via finite difference method," *Int. J. Appl. Phys. Math.*, vol. 4, no. 5, pp. 332–344, 2014. https://doi.org/10.7763/IJAPM.2014.V4.306

[23] G. Deepa and G. Murali, "Effects of viscous dissipation on unsteady MHD free convective flow with thermophoresis past a radiate inclined permeable plate," *Iran. J. Sci. Technol. (Sciences)*, pp. 379–388, 2014.

[24] G. Murali, A. Paul, and N. V. N. Babu, "Heat and mass transfer effects on an unsteady hydromagnetic free convective flow over an infinite vertical plate embedded in a porous medium with heat absorption," *Int. J. Open Probl. Compt. Math.*, vol. 8, no. 1, 2015. https://doi.org/10.12816/0010706

[25] N. V. N. Babu, A. Paul, and G. Murali, "Soret and Dufour effects on unsteady hydromagnetic free convective fluid flow past an infinite vertical porous plate in the presence of chemical reaction," *J. Sci. Arts*, vol. 15, no. 1, pp. 99–111, 2015. https://doi.org/10.12816/0010706

[26] M. Gundagani, "Unsteady MHD free convection viscous dissipative flow past an infinite vertical plate with constant suction and heat source/sink," *J. Sci. Arts*, vol. 15, no. 1, pp. 89–98, 2015.

[27] G. Murali, A. Paul, and N. V. N. Babu, "Numerical study of chemical reaction effects on unsteady mhd fluid flow past an infinite vertical plate embedded in a porous medium with variable suction," *Electron. J. Math. Anal. Appl.*, vol. 3, no. 2, pp. 179–192, 2015. https://doi.org/10.21608/EJMAA.2015.310762

[28] N. Babu, G. Murali, and S. M. Bhati, "Casson fluid performance on natural convective dissipative Couette flow past an infinite vertically inclined plate filled in porous medium with heat transfer, MHD and hall current effects," *Int. J. Pharm. Res.*, vol. 10, no. 4, 2018.

[29] D. Gadipally, M. Gundagani, and N. V. N. Babu, "Effects of thermal radiation and chemical reaction on unsteady hydromagnetic mixed convection flow past an infinite vertical plate," *J. Sci. Arts*, vol. 18, no. 3, pp. 763–776, 2018.

[30] G. Murali and N. V. N. Babu, "Convective MHD Jeffrey fluid flow due to vertical plates with pulsed fluid suction: A numerical study," *J. Comput. Appl. Mech.*, vol. 54, no. 1, pp. 36–48, 2023. https://doi.org/10.22059/JCAMECH.2023.351326.773